diversity

MDPI

*Article*

# Species Delimitation of *Argonauta* Paralarvae Reveals an Extensive Morphological Variability in the Northern Humboldt Current System

**Ximena Orosco [1,2], Patricia Ayón [2,3], Giovanna Sotil [1,4] and Jorge L. Ramirez [1,*]**

[1] Facultad de Ciencias Biológicas, Universidad Nacional Mayor de San Marcos, Cercado de Lima 15081, Peru; luz.orosco@unmsm.edu.pe (X.O.); gsotil@imarpe.gob.pe (G.S.)
[2] Laboratorio de Zooplancton e Ictioplancton, Instituto del Mar del Peru, Callao 07021, Peru; payon@imarpe.gob.pe
[3] Facultad de Ciencias Biológicas, Universidad Ricardo Palma, Santiago de Surco 15039, Peru
[4] Laboratorio de Genética Molecular, Instituto del Mar del Perú, Callao 07021, Peru
* Correspondence: jramirezma@unmsm.edu.pe

**Abstract:** Argonauts or *paper nautiluses* are pelagic octopod cephalopods with a cosmopolitan distribution in tropical and subtropical waters around the world. Unlike other species of octopus, these are characterized by the fact that the female has a shell that serves as the breeding chamber for the eggs. Over time, this structure has been used as a taxonomic diagnostic character, causing problems in the systematics of this genus, with around 50 synonymies reported. Only two species, *Argonauta argo* and *A. nouryi*, have been reported in the Northern Humboldt Current System; however, there is taxonomic uncertainty regarding these species, which is reflected in the paralarvae (the first stage of life after hatching). In the paralarvae, the chromatophore patterns are considered to be conservative and reliable taxonomic characteristics. The objective of this study is to demonstrate the extensive variability in the chromatophore arrangement of *Argonauta* paralarvae in the Northern Humboldt Current using DNA barcoding and five species delimitation models. Our results include up to 11 different paralarvae morphotypes according to the pattern of chromatophores (number and arrangement) and 2 shell morphotypes. Species delimitation methods divided the 13 *Argonauta* morphotypes into two consensus molecular taxonomic units (MOTUs), *A. argo* and *A. nouryi*. Additionally, the results revealed an extensive morphological variability in the paralarvae and female shells of *A. nouryi*, demonstrating the importance of molecular data in studies involving species with different life stages, especially when this extensive morphological variability obscures conventional analyses.

**Keywords:** argonauts; cephalopods; DNA barcoding; chromatophore; *paper nautilus*



**Citation:** Orosco, X.; Ayón, P.; Sotil, G.; Ramirez, J.L. Species Delimitation of *Argonauta* Paralarvae Reveals an Extensive Morphological Variability in the Northern Humboldt Current System. *Diversity* **2024**, *16*, 320. https://doi.org/10.3390/d16060320

Academic Editors: Xiaodong Zheng and Ran Xu

Received: 20 November 2023
Revised: 7 January 2024
Accepted: 8 January 2024
Published: 28 May 2024



## 1. Introduction

The Humboldt Current System, a cold-water current, extends along the west coast of South America from southern Chile (42°S) up to the Galapagos Islands near the equator [1]. The Northern Humboldt Current System (NHCS), the northern area facing Peru, represents less than 0.1% of the world's ocean surface but currently produces about 10% of the world's fish catch [2]. In this region, the most important fish are Peruvian anchovy *Engraulis ringens* (Jenyns, 1842), and the jumbo flying squid *Dosidicus gigas* (d'Orbigny, 1835) [3]. However, there are other species of ecological importance such as the cephalopod genus *Argonauta* (Linnaeus, 1758), which is an indicator of the approach of warm ocean waters to the coasts of the Peruvian Sea [4], especially during El Niño events.

Argonauts or *paper nautiluses* (Argonautidae) are a family of pelagic octopuses that inhabit tropical and temperate oceans of the world [5]. These group of octopuses are easily differentiated from benthic octopuses due to the presence of a shell called a *paper nautilus*, present only in females. This shell is secreted by the first pairs of arms and

functions as the breeding chamber for the eggs and their subsequent fertilization [6]. For many years, the morphological characteristics of these shells in adults have been used as a taxonomic characteristic with which to differentiate species [7–10]. However, this genus presents problems in the organization of its systematics around the world. Web platforms such as WORMS (htpp://www.marinespecies.ogr) (accessed on 23 September 2023), ITIS (htpp://www.itis.gov) (accessed on 23 September 2023), and BoldSystems (htpp://www.boldsystems.org) (accessed on 23 September 2023) show no consensus on the number of species in this molluscan group.

Adults present difficulties in not only taxonomic identification [6,11] but also in their first post-hatching life stages, known as paralarvae [12]. A specialized bibliography on the taxonomic aspects of paralarvae is lacking worldwide, especially for the Pacific Ocean. Some studies suggest that the chromatophore pattern is a conservative and reliable taxonomic characteristic [13,14]. Thus, the number and distribution of each chromatophore, the iridophore pattern, and the arm length formula are considered species-specific [11]. However, the analysis of these characters is problematic, not only because of their low abundance in zooplankton samples (typically between 1 and 5 individuals per net [15]), but also due to difficulties during the fixing of the paralarvae. For example, specimens tend to invert the mantle muscle when dragged in the net during zooplankton sampling collection, different chromatophores are discolored by the fixative, and appendages detach (arms and/or tentacles), hindering determination by conventional morphometric analysis [16]. Despite their small size, paralarvae are capable of evading high-speed sampler equipment [15], which further reduces the possibilities to study them.

For these reasons, the selection of alternative techniques such as DNA barcoding over conventional ones is necessary. This molecular identification tool uses a short and standardized section of the mitochondrial gene Cytochrome Oxidase I (COI) [17] and has been proven efficient in evaluating diversity in the marine ecosystem [18,19]. Recently, molecular data together with species delimitation methods were used to reveal the diversity of cephalopods [20–23].

Therefore, we used a DNA barcoding approach together with species delimitation methods to identify the *Argonauta* paralarva diversity in the NHCS, distinguishing molecular operational taxonomic units (MOTUs) and revealing the morphological variability in the number and arrangement of chromatophores. This work contributes to updating the list of species of the genus in the NHCS.

## 2. Materials and Methods

### *2.1. Sampling*

A total of 15 paralarvae and 1 juvenile of *Argonauta* were obtained from zooplankton samples collected using different nets (Figure 1, Table 1). The individuals were separated onboard and placed into 2 mL cryovials containing 96° ethanol and stored at 4 °C for one week. Additionally, two female adults with shells were collected via pelagic trawl during research cruises of the Instituto del Mar del Perú (IMARPE) (Table 1). Egg masses from these individuals were stored in 96° ethanol for molecular analysis.

**Table 1.** Paralarvae of *Argonauta* sampled along the Northern Humboldt Current System (NHCS) between 2017 and 2023.

| Barcode Accession Number | Sex | Dorsal Mantle Length (mm) | Latitude | Longitude | Net | Year |
|---|---|---|---|---|---|---|
| PMZPK063_20 | M | 1.1 | 8°5.954 S | 83°45.008 W | Bongo 300 µm | 2017 |
| PMZPK064_20 | M | 1.0 | 7°33.569 S | 82°49.057 W | Bongo 300 µm | 2017 |
| PMZPK065_20 | F | 1.2 | 7°3.598 S | 83°19.075 W | Bongo 300 µm | 2017 |
| PMZPK066_20 | F | 1.0 | 7°31.346 S | 84°6.873 W | Bongo 300 µm | 2017 |
| PMZPK070_20 | F | 1.2 | 6°39.534 S | 81°56.751 W | Bongo 300 µm | 2017 |

**Table 1.** *Cont.*

| Barcode Accession Number | Sex | Dorsal Mantle Length (mm) | Latitude | Longitude | Net | Year |
|---|---|---|---|---|---|---|
| PMZPK071_20 | F | 1.0 | 6°39.534 S | 81°56.751 W | Bongo 300 µm | 2017 |
| PMZPK072_20 | F | 1.7 | 6°40.1 | 82°38.677 W | Bongo 300 µm | 2017 |
| PMZPK073_20 | F | 1.0 | 6°0.039 S | 82°57.959 W | Bongo 300 µm | 2017 |
| PMZPK078_20 | F | 0.9 | 6°54.661 S | 81°41.04 W | Bongo 300 µm | 2017 |
| PMZPK079_20 | F | 0.8 | 8°011 S | 83°34.898 W | Bongo 300 µm | 2017 |
| PMZPK085_20 | F | egg mass | 13°28.921 S | 77°0.538 W | Pelagic trawl | 2019 |
| PMZPK086_20 | F | egg mass | 13°28.921 S | 77°0.538 W | Pelagic trawl | 2019 |
| PMZPK143-23 | - | 2.2 | 9°48.171 S | 80°08.640 W | IKMT | 2022 |
| PMZPK144-23 | - | 1.0 | 14° 4.001 S | 77°29.002 W | CUFES | 2019 |
| PMZPK145-23 | F | juvenile (3.5 mm) | 12°03.440 S | 77°10.0405 W | Bongo 300 µm | 2023 |
| PMZPK146-23 | - | 2.5 | 13°26.627 S | 78°12.331 W | Bongo 300 µm | 2019 |
| PMZPK147-23 | - | 1.0 | 10°44.882 S | 80°36.264 W | Bongo 300 µm | 2019 |
| PMZPK148-23 | - | 1.3 | 6°30.058 S | 82°10.967 W | Bongo 300 µm | 2019 |

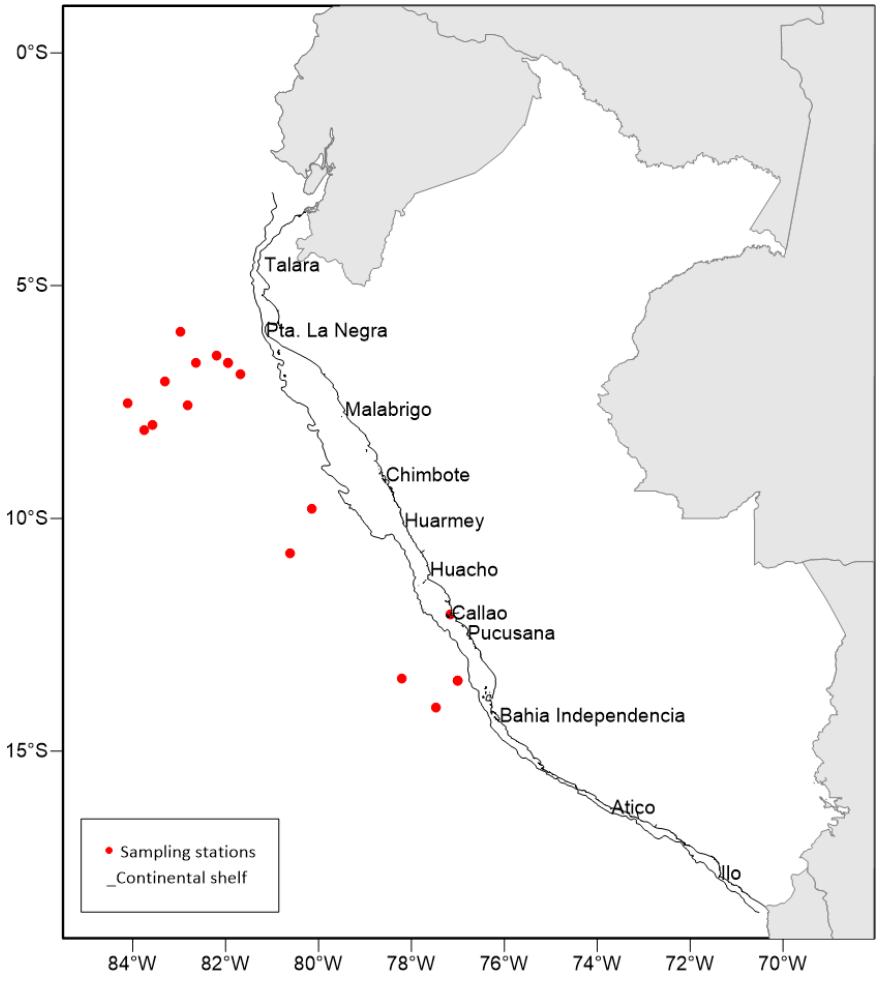


**Figure 1.** Sampling area of *Argonauta* paralarvae in the Northern Humboldt Current System (NHCS). The red dots are the zooplankton sampling stations (different nets), and the line parallel to the coast is the continental shelf.

### 2.2. Morphological Description

The morphological descriptions of the paralarvae were performed in specimens between 0.8 and 2.5 mm in dorsal mantle length (ML). The morphological determination was performed after consulting a specialized bibliography of cephalopod paralarvae [11,24–26]. The shells of females were identified according to Finn [6]. The ML was measured (mm) with a Nikon SMZ 1270 stereomicroscope equipped with a digital camera and NIS Element D v. 4.13 image capture software. The funnel-locking apparatus was reviewed. Specimens were sexed due to sexual dimorphism. Males have a hectocotylized third arm that is wrapped in a bag called a "pouch". Chromatophore pattern (number, position, and formula) of the DHCP (dorsal head chromatophore pattern), VHCP (ventral head chromatophore pattern), dorsal mantle (DM), ventral mantle (VM), dorsal eye (DE), ventral eye (VE), digestive gland (DG), funnel, arms, and hectocotylus (for males) on each morphotype were described according to De Silva-Dávila [24] (Figure 2). Likewise, diagrams (drawings) were made using a camera lucida suitable for the stereomicroscope. The voucher specimens were deposited in the scientific collection of the Laboratorio de Zooplancton y Producción Secundaria of IMARPE.

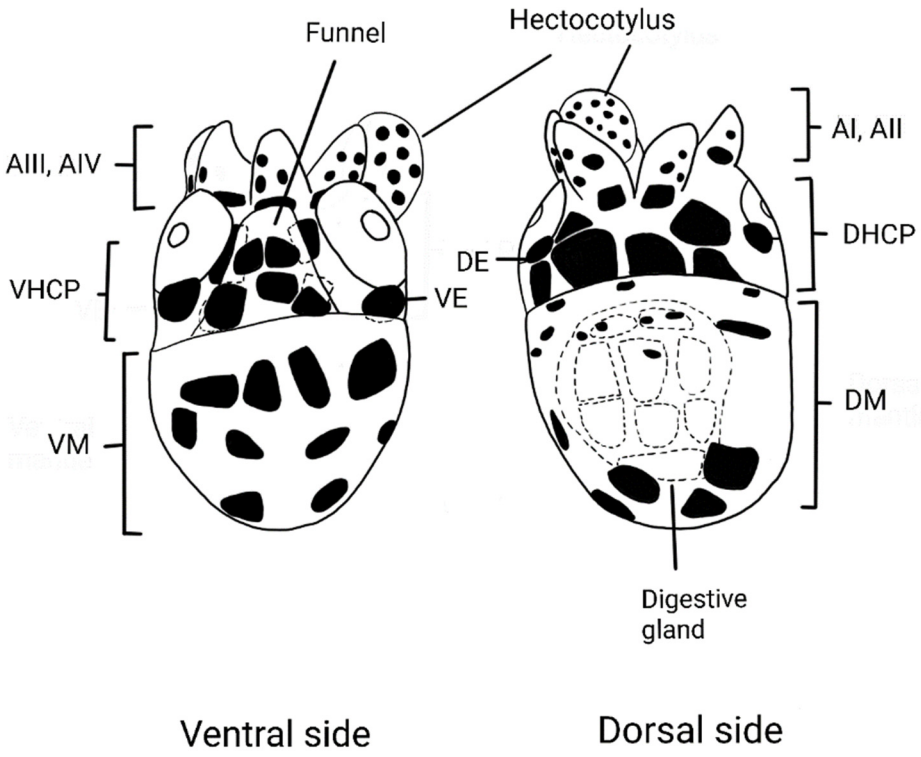


**Figure 2.** *Argonauta* paralarva chromatophore pattern diagram (ML: 1 mm): dorsal head chromatophore pattern (DHCP), ventral head chromatophore pattern (VHCP), dorsal mantle (DM), ventral mantle (VM), dorsal eye (DE), ventral eye (VE), digestive gland (DG), funnel, arms (AI-AIV), and hectocotylus (for males).

### 2.3. DNA Extraction, Amplification and Sequencing

DNA extraction was performed using the HotSHOT method [27]. Tissues were transferred into 0.2 mL microtubes containing 50 µL of alkaline lysis buffer (25 mM NaOH, 0.2 mM EDTA, pH 8.0) and were ground using a sterile micropipette tip. The samples were incubated at 95 °C for 30 min, followed by 4 °C for 4 min in a thermocycler. Then, 50 µL of neutralizing solution (40 mM Tris-HCl, pH 5.0) was added, followed by a vortex (to homogenize) and a spin in a mini-centrifuge. All samples were stored at 4 °C for use directly in the PCR. For species identification, the cytochrome oxidase subunit I (COI) gene of mitochondrial DNA (mtDNA) was amplified with the primers ZplankF1_t1/ZplankR1_t1 [28].

The PCR was performed using 1X of Taq buffer, 0.25 mM of each dNTP, 0.4 mM of each primer, 2.5 mM of $MgCl_2$, 0.5 U of Vazyme Taq DNA polymerase, and 2 µL of DNA in 15 µL of the final reaction volume. Other PCRs were performed using the HotStartTaq Plus Master Mix kit (QIAGEN). The PCR conditions were an initial denaturation at 95 °C for 5 min, followed by 36 cycles at 95 °C for 40 s, 45 °C for 50 s, and 72 °C for 1 min, with a final extension of 72 °C for 7 min. All reactions were evaluated via electrophoresis in 1% agarose gels, and amplified products with the expected size were then bidirectionally sequenced on a genetic analyzer ABI 3500 (Applied Biosystems) using both a commercial service and at IMARPE. The contigs were assembled using the software CodonCode Aligner v. 6.0.2 (Codon Code Corporation, Dedham, MA, USA). Primer sequences and bad-quality regions were trimmed. The consensus sequences and all specimen data were deposited in the dataset BOLD (https://www.boldsystems.org/, accessed on 6 January 2024) under dataset code DS-ARGNT.

### *2.4. Species Delimitation*

To infer MOTUs using different species delimitation methods, our sequences were combined with thirteen COI sequences from three *Argonauta* species from different oceans (Accession numbers AF000028, MT216541, MT216542, MK034303, AB191273, ON367817, OP132805, OP132808, OP132809, OP132810, LC596061, KY649285, and OR234732) retrieved from GenBank (www.ncbi.nlm.nih.gov/genbank/, accessed on 6 January 2024).

The thirty-one DNA sequences (627 pb) were aligned in the FASTA format, and five species delimitation methods were performed using pipeline SPdel [29]: ABGD (automatic barcode gap discovery) [30], ASAP (assemble species by automatic partitioning) [31], GMYC (generalized mixed yule coalescent approach) [32], bPTP (Bayesian Poisson tree processes) [33], and mPTP (multi-rate Poisson tree processes) [33]. For bPTP and mPTP methods, an ultrametric tree was generated using BEAST v2.5 [34], with a log-normal relaxed clock model and HKY+G substitution model suggested by the Bayesian Information Criterion (AIC) in jModeltest 2 [35]. The analysis was implemented with 100,000,000 MCMC generations and with a burn-in of 10%. Consensus MOTUs were generated by comparing the five delimitation methods. Values of intragroup and intergroup Kimura 2-parameter (K2P) genetic distances for nominal species and consensus MOTUs were calculated using SPdel.

## 3. Results

### *3.1. Morphological Determination*

After the morphological revision, 13 different morphotypes were determined, including 11 different chromatophore patterns ($n$ = 16; *Argonauta* M1 ($n$ = 2), *Argonauta* M5 ($n$ = 1), *Argonauta* M6 ($n$ = 1), *Argonauta* M7 ($n$ = 2), *Argonauta* M8 ($n$ = 1), *Argonauta* M10 ($n$ = 1), *Argonauta* M12 ($n$ = 1), *Argonauta* M13 ($n$ = 1), *Argonauta* M15 ($n$ = 1), Argonauta M17 ($n$ = 1), and *Argonauta* M18 ($n$ = 4)). The two female adults were identified as *A. nouryi* based on shell morphology. In accordance with the morphotypes reported by Finn [6], the females exhibited two different shell morphotypes *A. nouryi* shell type I (st_I), ($n$ = 1) and *A. nouryi* shell type II (st_II), ($n$ = 1) (Figure 3k,i and Table 2),

**Table 2.** Morphological and meristic characteristics of the *Argonauta* paralarvae collected in the NHCS. M = male; F = female. The chromatophore pattern is related to the number of chromatophores. (The DHCP, VHCP, dorsal mantle, ventral mantle, and funnel columns are read from top to bottom, each row separated with a "+" sign. In the arms column, the reading extends from the base to the distal part of the appendages. In the dorsal and ventral eye area columns, the number inside the parentheses refers to the number for both eyes. In the digestive gland and hectocotyl columns, the number refers to the total chromatophore count.)

| Barcode Accession Number | Morphotype | ML (mm) | Sex | Chromatophore Pattern | | | | | | | | | |
|---|---|---|---|---|---|---|---|---|---|---|---|---|---|
| | | | | DHCP | VHCP | DM | VM | DE | VE | DG | Funnel | Arms | Hectocotyl |
| PMZPK145-23 | M1 | 3.5 | F | - | - | - | - | - | - | - | 1 + 2 | BI:1b + 19dr/BII:1b + 11dr/BIII:1b + 11dr/BIV:1b + 14dr | |
| PMZPK146-23 | M1 | 2.5 | | 2 + 4 | 2 + 2 | - | - | 2(2) | 1(2) | - | 1 + 2 | - | |
| PMPZK063-20 | M5 | 1.1 | M | 2 + 4 | 2 + 2 | 4 + 4 + 2 + 1 | 4 + 3 + 3 + 2 + 1 | 2(2) | 1(2) | 9 | 2 | BI-BIII:1b + 1/BIV:1b + 1 + 1 | 10 |
| PMPZK066-20 | M6 | 1 | F | 2 + 4 | 2 + 2 | 5 + 2 + 1 | 5 + 3 + 2 + 2 + 2 | 1(2) | 1(2) | 8 | 1 | BI-BIII: 1b/BIV: 1b + 1 | - |
| PMPZK064-20 | M7 | 1 | M | 2 + 4 | 2 + 2 | 4 + 4 + 2 + 1~ | 5 + 1 * + 4 + 2 + 1 | 2(2) | 1(2) | 10 | 1 + 2 + 1 * | BI-BIII: 1b + 1 + 1dr (d)/BIV: 1b + 2 + 1dr(d) | 33 |
| PMPZK147-23 | M7 | 1.3 | | 2 + 4 | 2 + 2 | - | - | 2(2) | 1(2) | - | 1 + 1 + 2 | - | |
| PMPZK148-23 | M8 | 1 | | 2 + 4 | 2 + 2 | - | - | 2(2) | 1(2) | - | 2 + 1 + 2 | - | |
| PMPZK071-20 | M10 | 1 | F | 2 + 4 | 2 + 2 | 4 + 2 + 2 + 1 | 4 + 3 + 5 + 1 + 2 | 2(2) | 1(2) | 8 | 1 + 2 + 2 | BI:1b + 1 * + 1dr(d)/BII:1b + 1/BIII:1b/BIV: 1b + 1 | 10 |
| PMPZK072-20 | M12 | 1.7 | F | 2 + 4 | 2 + 2 | 5 + 2 + 1 | 54 + 1 + 2 | 2(2) | 1(2) | 10 | 1 + 2 + 1 | BI- BIII: 1b/BIV: 1b + 1 | - |
| PMPZK070-20 | M13 | 1.2 | F | 2 + 4 | 2 + 2 | 4 + 2 + 2 + 1 + 2 | 4 + 2 + 3 + 2 | 2(2) | 1(2) | 10 | 1 + 1 | BI: 1b + 1 + 1dr(d)/BII-BIII: 1b + 1/BIV:1b + 1 + 1 | - |
| PMPZK078-20 | M15 | 0.9 | F | 2 + 4 | 2 + 2 | 5 + 1 * + 2 | 4 + 3 + 2 + 1 | 2(2) | 1(2) | 11 | 2 + 1 | BI-BIII: 1b/BIV: 1b + 1 | - |
| PMPZK073-20 | M17 | 1 | F | 2 + 4 | 2 + 2 | 3 + 7 + 1 * + 2 + 1 | 4 + 4 + 2 | 1(2) | 1(2) | 9 | 2 + 1 + 2 | BI: 1b + 1 + 1dr(d)/BII-BIII: 1b + 1/BIV: 1b + 1dr + 1 | - |
| PMPZK065-20 | M18 | 1.2 | F | 2 + 4 | 2 + 2 | 4 + 3 + 2 | 4 + 3 + 2 | 2(2) | 1(2) | 9 | 2 + 2 | BI & BIV: 1b + 1/BII-BIII: 1b | - |
| PMPZK079-20 | M18 | 0.8 | F | 2 + 4 | 2 + 2 | 4 + 2 + 1 | 4 + 3 + 1 + 2 | 1(2) | 1(2) | 9 | 2 + 2 | BI & BIV 1b + 1/BII-BIII: 1b | - |
| PMPZK143-23 | M18 | 2.2 | F | 2 + 4 | 2 + 2 | 5 + 4 + 4 + 3 + 2 + 1 | 5 + 5 + 4 + 5 | 2(2) | 1(2) | - | 2 + 2 | BI: 1b + 4dr/BII: 1b + 4sr/BIII: 1b + 3sr/BIV: 1b + 5dr | - |
| PMPZK144-23 | M18 | - | | 2 + 4 | 2 + 2 | - | - | 2(2) | 1(2) | - | 2 + 2 | - | - |
| PMPZK086-20 | st_I | | F | Egg mass of female with shell type I (Finn 2013) | | | | | | | | - | - |
| PMPZK085-20 | st_II | | F | Egg mass of female with shell type II (Finn 2013) | | | | | | | | - | - |

Note: b: at base, d: distal, dr: double row, sr: simple row, *: only found on one of the sides (considering the bilateral symmetry), (): in total from each eye.

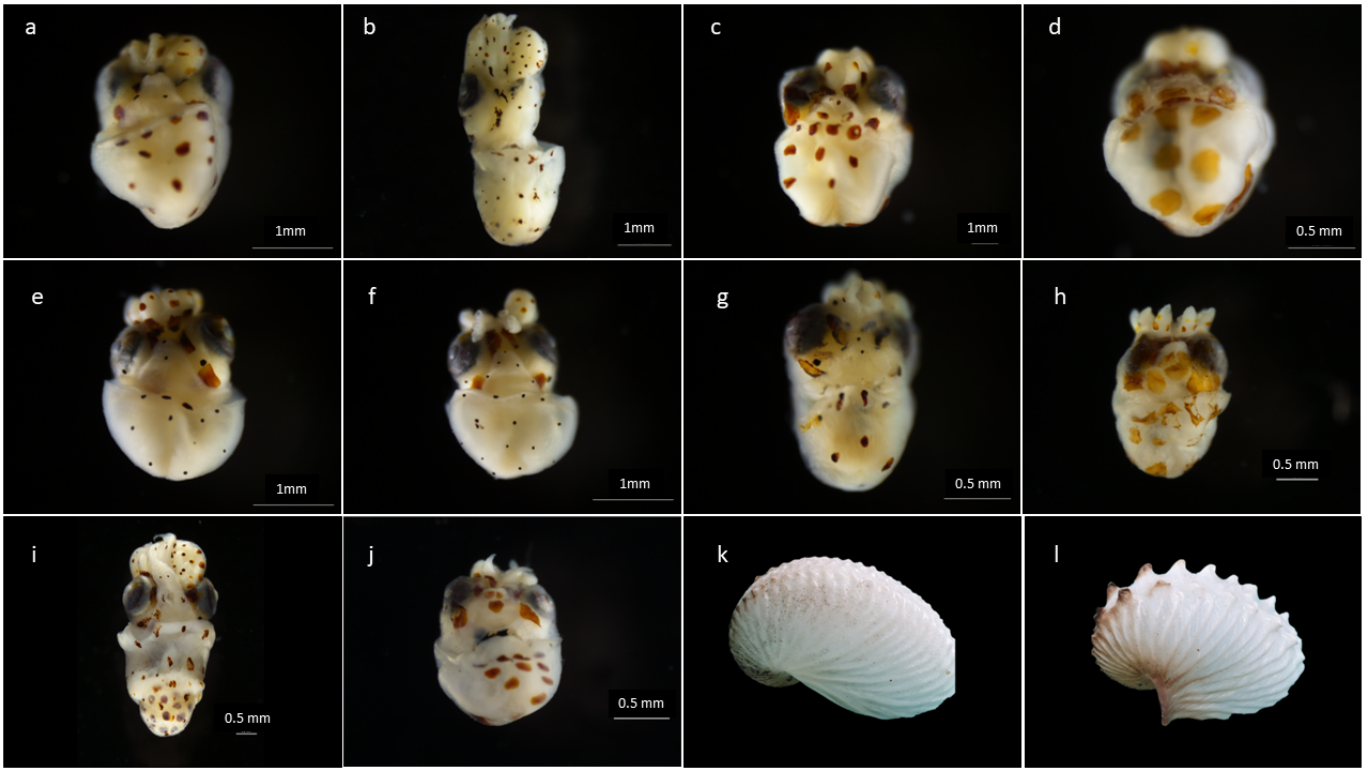


**Figure 3.** *Argonauta* paralarvae, ventral side (**a**–**j**) and shell, lateral side (**k**,**l**) of an adult female collected in this study. Sample codes: (**a**) PMZPK063-20 (M5), (**b**) PMPZK064-20 (M7), (**c**) PMPZK065-20 (M18), (**d**) PMPZK066-20 (M6), (**e**) PMPZK070-20 (M13), (**f**) PMZPK071-20 (M10), (**g**) PMPZK072-20 (M12), (**h**) PMPZK073-20 (M17), (**i**) PMPZK076-20, (**j**) PMPZK078-20 (M15), (**k**) PMPZK086-20 (st_I) and (**l**) PMPZK085-20 (st_II).

The most variable chromatophore pattern was observed in the funnel, by which individuals were delimited into different morphotypes (Table 2, Figure 4). The chromatophore arrangements that remained consistent in all organisms were the DHCP (2 + 4) and VHCP (2 + 2). The number of chromatophores in the digestive gland ranged from 8 to 11 in all paralarvae, and only one chromatophore was observed at the base of each arm (1b). Due to fixation, the arrangement, number, and disposition of the chromatophores on the dorsal and ventral sides of the mantle and in the hectocotylus could be observed in only a few individuals.

For individuals between 0.8 and 2.2 mm, the number of VE chromatophores remained the same (one in each eye). However, the number of chromatophores on the dorsal side (DE) varied. In *Argonauta* M6 (PMPZK066-20), *Argonauta* M17 (PMPZK073-20), and *Argonauta* M18 (PMPZK079-20), only one chromatophore associated with the eye was observed, while the other morphotypes described showed two. For the juvenile (3.5 mm) *Argonauta* M1 (PMZPK145-23), only the oldest chromatophores (brown) in the funnel were considered (1 + 2) as, in the other parts of the body, it was impossible to establish a pattern due to the number of new chromatophores that appeared (orange).

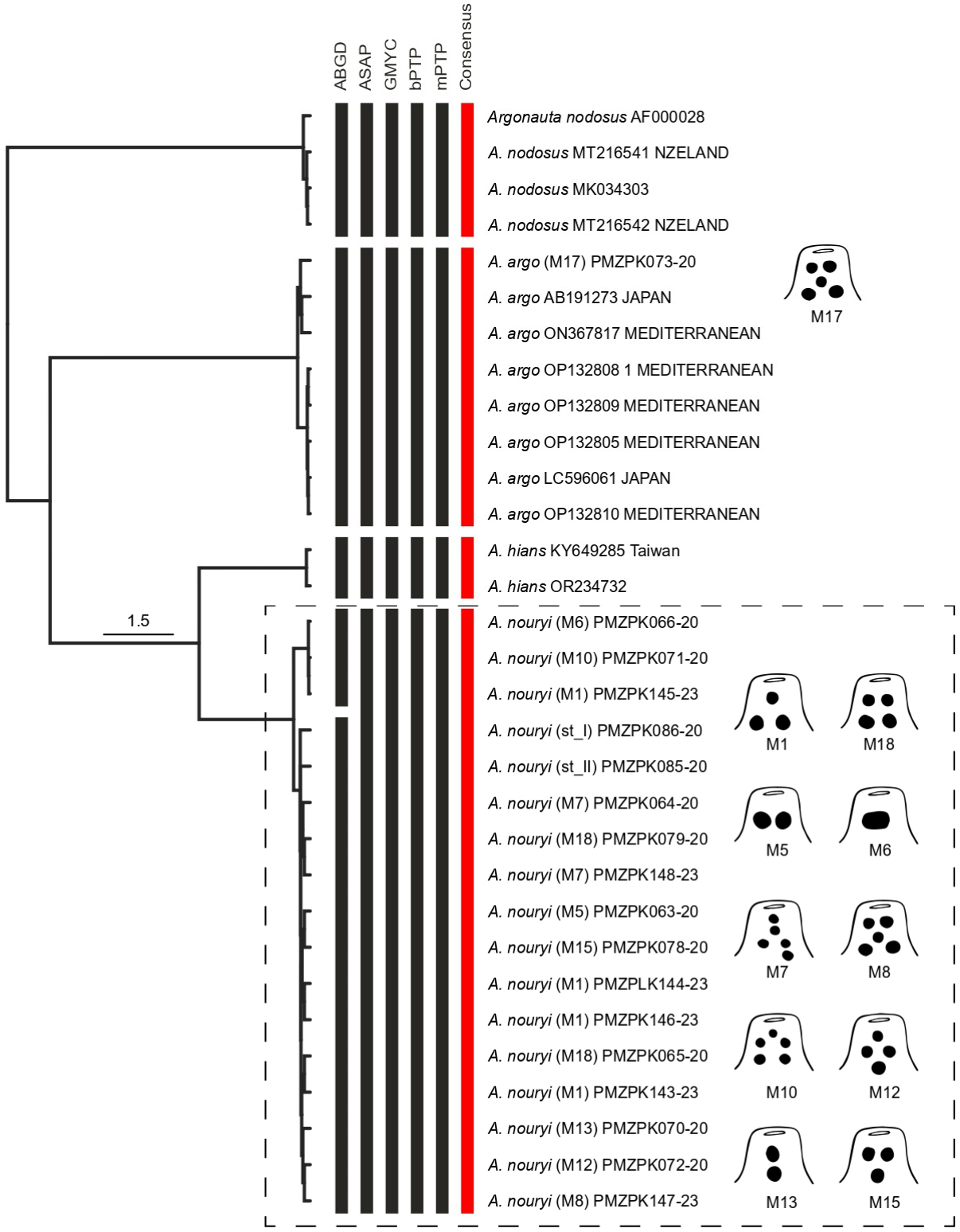


**Figure 4.** Bayesian tree showing the clustering of the MOTUs resulting from ABGD, ASAP, bPTP, and mPTP analysis, and consensus MOTUs. The black vertical bars represent the numbers of species delimited by ABGD, ASAP, GMYC, bPTP, and mPTP methods; and the red vertical bars represent consensus MOTUs. The scale bar indicates the nucleotide substitutions per site. The codes in parentheses refer to the described morphotype of *Argonauta*, and the subsequent code to the barcode accession number. Note the different morphotypes (schemes) corresponding to the *A. nouryi* MOTU.

### 3.2. DNA Barcode Analysis and Species Delimitation

We obtained 18 sequences from the 13 morphotypes. The final alignment of COI sequences resulted in 627 bp with 102 parsimony-informative sites. The ABGD, ASAP, GYMC, bPTP, and mPTP analyses resulted in four MOTUs (Figure 4). SPdel summarized the different delimitation results in four consensus MOTUs (Figure 4). From the 13 morphotypes, the individual determined as *Argonauta* M17 was grouped with *Argonauta argo* from Japan and the Mediterranean Sea in MOTU 01. Meanwhile, the other 12 morphotypes were grouped into MOTU 04, including two female adults of *A. nouryi* (Figure 4). The other two MOTUs corresponded to *Argonauta nodosus* and *Argonauta hians* from New Zealand and Taiwan, respectively. The genetic intra-MOTU and inter-MOTU distances are shown in Table 3. The highest maximum intra-MOTU distance was 0.97% for MOTU 04 (*A. nouryi*) and the lowest minimum inter-MOTU distance was 4.63% between MOTU 02 (*A. hians*) and MOTU 04 (*A. nouryi*).

**Table 3.** Genetic K2-P distance of the MOTUs of *Argonauta*: mean intra-MOTU divergence (Mean), maximum intra-MOTU divergence (Max), nearest neighbor (NN), and distance to the nearest neighbor (DtoNN).

| Consensus MOTUs | Mean | Max | NN | DtoNN |
|---|---|---|---|---|
| MOTU 01 (*A. argo)* | 0.22 | 0.64 | MOTU 04 | 8.80 |
| MOTU 02 (*A. hians*) | 0.16 | 0.16 | MOTU 04 | 4.63 |
| MOTU 03 (*A. nodosus)* | 0.16 | 0.32 | MOTU 02 | 11.01 |
| MOTU 04 (*A. nouryi*) | 0.28 | 0.97 | MOTU 02 | 4.63 |

## 4. Discussion

Our results supported four consensus MOTUs corresponding to the four known nominal species: *A. argo*, *A. hians*, *A. nodosus*, and *A. nouryi* [6]. From these, two species of the *Argonauta* genus are considered to be distributed in the Northern Humboldt Current System at the adult level: *A. argo* and *A. nouryi* [36]. Previous studies also reported the presence of *A. hians* [36–38]; however, Finn reported *A. hians* as being restricted to the Atlantic and Indian oceans, and Arabian, Chinese, and Philippine seas after a global review of the systematics and distribution of the genus [6]. At the paralarva level in the NHCS, it had previously only been possible to identify different morphotypes as *Argonauta* spp. [4]. Our results show the presence of the two species *A. argo* and *A. nouryi* in the NHCS, in accordance with Finn [6], the latter being a new public BIN (BOLD:ABA3205) for the BOLDSystem database.

The paralarvae characterized herein were grouped into two consensus MOTUs: MOTU 01 (*A. argo*) and MOTU 04 (*A. nouryi*). The MOTU 01 was identified as *A. argo* using sequences from previous studies [39], including sequences from adult individuals [39]. The MOTU 04 was identified as *A. nouryi* based on the two female adults herein sequenced. In these MOTUs, paralarvae with different dispositions and numbers of chromatophores in the funnel clustered together, showing high morphological variability. There are many studies that report and analyze the abundance, frequency, and spatial distribution associated with different oceanographic conditions of *A. nouryi* [40,41]. However, there is no morphological description of its paralarvae, only references to the fact that it was previously named *Argonauta boettgeri* [24] in the Mexican Pacific Ocean [42], with an arrangement of 1 + 2 in the funnel, 2 + 2 in the VHCP, and 2 + 4 in the DHCP. Our results for *A. nouryi* show a wide variability in the number and arrangement of chromatophores in the funnel: 2 + 4 in the DHCP, 2 + 2 in the VHCP, 02 chromatophores in each eye (dorsal side), and between 8 and 11 in the digestive gland (Table 2). This highlights the significant challenge of taxonomic determination based solely on morphological characteristics, especially the chromatophore pattern. This complexity increases when we consider that some ancient descriptions did not mention the chromatophore arrangement [43]. However, over the years, some authors have incorporated this information into descriptions, such as that of *A.*

*argo* (~1 mm) with a 2 + 2 arrangement in the funnel, with 2 chromatophores on the dorsal side of the head [11,25], and 2 + 4 DHCP [24]. In the present work, *A. argo* is reported with a chromatophore arrangement of 2 + 1 + 2 in the funnel, 2 + 4 in the DHCP, 2 + 2 in the VHCP, 1 chromatophore in each eye (dorsal side), and 9 in the digestive gland, also showing morphological variability. Descriptions of the paralarvae of *A. hians* (1.0 mm) are scarcer [11,43,44], where some authors describe2 + 2 in the funnel and in the VHCP [24], an arrangement of 4 chromatophores (rectangle shape) on the dorsal side of the head [26], and 4 + 4 in the DHCP [24,40–42]. Although the paralarvae of *Argonauta nodosus* were reported by [45,46], there is no morphological description of them.

Cephalopod chromatophores comprise an elastic saccule containing pigment, to which a set of diagonally striped radial muscles are attached, each with its associated nerves and glial cells [47,48]. As chromatophores are neuronally controlled, an individual can select and display one particular body pattern among many at any time (e.g., at fixation) [49], hindering taxonomic work. In some groups, such as the Loliginidae family, chromatophores are considered good taxonomic characters that allow the identification of larval and juvenile stages [50–52]. However, our results show that in *Argonauta*, the observed chromatophores patterns are more variable than previously reported, including overlapping patterns. Future studies including a large number of individuals of each species are required to determine the variability of chromatophore patterns. This involves seeking constant and repeatable patterns and assessing whether they could be considered to be a taxonomic characteristic of *Argonauta*.

The shell of the female *Argonauta* is not a true mollusk shell; it is a secondary structure of calcite secreted by networks at the distal ends of the first pair of (dorsal) arms [53]. Although these shells were used in the past to delimit species of this genus, it is now known that they cannot be used for this purpose since they present a wide plasticity in their shape [6]. In particular, the shells of *A. nouryi* present a dramatic variation, also observed in this study, where the individuals with the type I shell (PMZPK086-20, Figure 3k), with thin ribs and without ears (the conventional shell of *A. nouryi*), and the type II shell (PMZPK085-20, Figure 3l), with larger keel tubercles and larger ears (characteristics historically attributed to the synonym *Argonauta cornutus*) [6], were grouped in the same MOTU (MOTU 04) of *A. nouryi*.

These results confirm the importance of implementing molecular tools such as DNA barcoding and bioinformatics tools like single-locus species delimitation methods. Furthermore, our results highlight the importance of integrating molecular data into studies involving species with different life stages, especially when extensive morphological variability hinders conventional taxonomic determination. In addition, the application of these results will allow us to practice better ecologic management of these species, especially in the case of *Argonauta*, whose paralarvae play the role of indicator species for the approach of warm oceanic waters toward the coast in El Niño events in the NHCS [4].

**Author Contributions:** Conceptualization, X.O., P.A. and J.L.R.; methodology, X.O., P.A., G.S. and J.L.R.; formal analysis, X.O., P.A. and J.L.R.; investigation, X.O. and J.L.R.; Supervision, P.A. and J.L.R.; writing—original draft preparation, X.O.; writing—review and editing, X.O., P.A., G.S. and J.L.R. All authors have read and agreed to the published version of the manuscript.

**Funding:** This research was supported by the Consejo Nacional de Ciencia, Tecnología e Innovación Tecnológica (CONCYTEC), Peru (Círculo de Investigación 023-2016-FONDECYT), PpR-137 Oceanografia and PpR-Meta 03 Desarrollo Tecnológico, Instituto del Mar del Perú (IMARPE), Ministerio de la Producción.

**Institutional Review Board Statement:** Not applicable.

**Informed Consent Statement:** Not applicable.

**Data Availability Statement:** Data are contained within the article.

**Acknowledgments:** We are grateful to Manuel Elías Gutierrez and Alma García Morales of the Barcode of Life Laboratory of El Colegio de la Frontera Sur (ECOSUR), Chetumal, México, for the support provided in their facilities for the training of DNA barcoding techniques.

**Conflicts of Interest:** The authors declare no conflict of interest.

## References

1. Thiel, M.; Macaya, E.; Acuña, E.; Arntz, W.; Bastias, H.; Brokordt, K.; Camus, P.; Castilla, J.; Castro, L.; Cortés, M.; et al. The Humboldt Current System of Northern and Central Chile. In *Oceanography and Marine Biology*; CRC Press: Boca Raton, FL, USA, 2007; Volume 45, pp. 195–344.
2. Chavez, F.P.; Bertrand, A.; Guevara-Carrasco, R.; Soler, P.; Csirke, J. The Northern Humboldt Current System: Brief History, Present Status and a View towards the Future. *Prog. Ocean.* **2008**, *79*, 95–105. [CrossRef]
3. Csirke, J.; Argüelles, J.; Alegre, A.; Ayón, P.; Bouchon, M.; Castillo, G.; Castillo, R.; Cisneros, R.; Guevara-Carrasco, R.; Lau, L.; et al. Biología, Estructura Poblacional y Pesquería de Pota o Calamar Gigante (*Dosidicus gigas*) En El Perú. *Bol. Inst. Mar. Perú* **2018**, *33*, 302–364.
4. Orosco, X.; Ayón, P. Variación de Paralarvas de Cefalópodos Asociada a Condiciones Oceanográficas En La Región Norte Del Sistema de La Corriente de Humboldt. *Bol. Inst. Mar. Perú* **2022**, *37*, 256–270. [CrossRef]
5. FAO. *Cephalopods of the World: An Annotated and Illustrated Catalogue of Cephalopod Species Known to Date*; Jereb, P., Roper, C.F.E., Norman, M.D., Finn, J.K., Eds.; Food and Agriculture Organization of the United Nations: Rome, Italy, 2016; Volume 3. ISBN 9789251079898.
6. Finn, J.K. Taxonomy and Biology of the Argonauts (Cephalopoda: Argonautidae) with Particular Reference to Australian Material. *Molluscan Res.* **2013**, *33*, 143–222. [CrossRef]
7. Sasaki, M. Report on Cephalopod Collected during 1906 by The United States Bureau of Fisheries Steaivier "Albatross" in the Northwestern Pacific. *Proc. U. S. Natl. Mus.* **1920**, *57*, 163–203. [CrossRef]
8. Robson, G.C. XXXIX.—Notes on the Cephalopoda.—No. 16. On the Variation, Eggs, and Ovipository Habits of Floridan Octopods. *Ann. Mag. Nat. Hist.* **1932**, *10*, 368–374. [CrossRef]
9. Voss, G.L. The Cephalopoda Obtained by: The Harvard-Havana Expedition off the Coast of Cuba in 1938-39. *Bull. Mar. Sci.* **1955**, *5*, 81–115.
10. Nesis, K.N. *Cephalopods of the World*; T.F.H. Publications: Neptune, NJ, USA, 1987.
11. Sweeney, M.J.; Roper, C.F.E.; Mangold, K.M.; Clarke, M.R.; Boletzky, S.V. (Eds.) *Smithsonian Contributions to Zoology "Larval" and Juvenile Cephalopods: A Manual for Their Identification*; Smithsonian Institution Press: Washington, DC, USA, 1992; Volume 513.
12. Young, R.E.; Harman, R.F. "Larva", "Paralarva" and "Subadult" in Cephalopod Terminology. *Malacologia* **1988**, *29*, 201–207.
13. Young, R.E.; Harman, R.F.; Hochberg, F.G. Octopodid Paralarvae from Hawaiian Waters. *Veliger* **1989**, *32*, 152–165.
14. Vidal, É.A.G.; Fuentes, L.; da Silva, L.B. Defining Octopus Vulgaris Populations: A Comparative Study of the Morphology and Chromatophore Pattern of Paralarvae from Northeastern and Southwestern Atlantic. *Fish. Res.* **2010**, *106*, 199–208. [CrossRef]
15. Vecchione, M. Juvenile Ecology. In *Cephalopod Life Cycles*; Boyle, P.R., Ed.; Academic Press: London, UK, 1987; Volume 2, p. 475.
16. De Silva-Dávila, R.; Hochberg, F.G.; Lindgren, A.R.; del Carmen Franco-Gordo, M. Paralarval Development, Abundance, and Distribution of *Pterygioteuthis hoylei* (Cephalopoda: Oegopsida: Pyroteuthidae) in the Gulf of California, México. *Molluscan Res.* **2013**, *33*, 50–64. [CrossRef]
17. Hebert, P.D.N.; Cywinska, A.; Ball, S.L.; DeWaard, J.R. Biological Identifications through DNA Barcodes. *Proc. R. Soc. B Biol. Sci.* **2003**, *270*, 313–321. [CrossRef]
18. Ramirez, J.L.; Rosas-Puchuri, U.; Cañedo, R.M.; Alfaro-Shigueto, J.; Ayon, P.; Zelada-Mázmela, E.; Siccha-Ramirez, R.; Velez-Zuazo, X. DNA Barcoding in the Southeast Pacific Marine Realm: Low Coverage and Geographic Representation despite High Diversity. *PLoS ONE* **2020**, *15*, e0244323. [CrossRef] [PubMed]
19. Ramirez, J.L.; Nuñez-Rodriguez, D.; Britzke, R.; Siccha-Ramirez, R.; Ramírez, R. DNA Barcoding for Assessing Biodiversity. In *Conservation Genetics in the Neotropics*; Pedro, M.G., Jr., Ed.; Springer International Publishing: Sao Carlos, Brazil, 2023; pp. 21–45.
20. Fernández-Álvarez, F.; Sánchez, P.; Villanueva, R. Morphological and Molecular Assessments of Bobtail Squids (Cephalopoda: Sepiolidae) Reveal a Hidden History of Biodiversity. *Front. Mar. Sci.* **2021**, *7*, 632261. [CrossRef]
21. Ibáñez, C.M.; Fenwick, M.; Ritchie, P.A.; Carrasco, S.A.; Pardo-Gandarillas, M.C. Systematics and Phylogenetic Relationships of New Zealand Benthic Octopuses (Cephalopoda: Octopodoidea). *Front. Mar. Sci.* **2020**, *7*, 182. [CrossRef]
22. Sales, J.B.d.L.; Rodrigues-Filho, L.F.d.S.; Ferreira, Y.d.S.; Carneiro, J.; Asp, N.E.; Shaw, P.W.; Haimovici, M.; Markaida, U.; Ready, J.; Schneider, H.; et al. Divergence of Cryptic Species of Doryteuthis Plei Blainville, 1823 (Loliginidae, Cephalopoda) in the Western Atlantic Ocean Is Associated with the Formation of the Caribbean Sea. *Mol. Phylogenet. Evol.* **2017**, *106*, 44–54. [CrossRef]
23. Xu, R.; Lü, Y.; Tang, Y.; Chen, Z.; Xu, C.; Zhang, X.; Zheng, X. DNA Barcoding Reveals High Hidden Species Diversity of Chinese Waters in the Cephalopoda. *Front. Mar. Sci.* **2022**, *9*, 830381. [CrossRef]
24. De Silva-Dávila, R. *Paralarvas de Cefalópodos En El Golfo de California, México*; Universidad de Guadalajara-CUCSUR: San Patricio Melaque, México, 2013.
25. Zaragoza, N.; Quetglas, A.; Moreno, A. *Identification Guide for Cephalopod Paralarvae from the Mediterranean Sea*; International Council for the Exploration of the Sea: Copenhagen, Denmark, 2015.

26. Sukhsangchan, C.; Sunthornket, P.; Phuynoi, S. Morphological Characteristics of Paralarvae of Cephalopods Found in Thai Waters. *Mar. Biodivers.* **2017**, *47*, 639–645. [CrossRef]
27. Montero-Pau, J.; Gómez, A.; Muñoz, J. Application of an Inexpensive and High-Throughput Genomic DNA Method for the Molecular Ecology of Zooplanktonic Eggs. *Limnol. Ocean. Methods* **2008**, *6*, 218–222. [CrossRef]
28. Prosser, S.; Martínez-Arce, A.; Elías-Gutiérrez, M. A New Set of Primers for COI Amplification from Freshwater Microcrustaceans. *Mol. Ecol. Resour.* **2013**, *13*, 1151–1155. [CrossRef]
29. Ramirez, J.L.; Valdivia, P.; Rosas-Puchuri, U.; Valdivia, N.L. SPdel: A Pipeline to Compare and Visualize Species Delimitation Methods for Single-Locus Datasets. *Mol. Ecol. Resour.* **2023**, *23*, 1959–1965. [CrossRef] [PubMed]
30. Puillandre, N.; Lambert, A.; Brouillet, S.; Achaz, G. ABGD, Automatic Barcode Gap Discovery for Primary Species Delimitation. *Mol. Ecol.* **2012**, *21*, 1864–1877. [CrossRef] [PubMed]
31. Puillandre, N.; Brouillet, S.; Achaz, G. ASAP: Assemble Species by Automatic Partitioning. *Mol. Ecol. Resour.* **2021**, *21*, 609–620. [CrossRef] [PubMed]
32. Fujisawa, T.; Barraclough, T.G. Delimiting Species Using Single-Locus Data and the Generalized Mixed Yule Coalescent Approach: A Revised Method and Evaluation on Simulated Data Sets. *Syst. Biol.* **2013**, *62*, 707–724. [CrossRef] [PubMed]
33. Zhang, J.; Kapli, P.; Pavlidis, P.; Stamatakis, A. A General Species Delimitation Method with Applications to Phylogenetic Placements. *Bioinformatics* **2013**, *29*, 2869–2876. [CrossRef] [PubMed]
34. Bouckaert, R.; Heled, J.; Kühnert, D.; Vaughan, T.; Wu, C.H.; Xie, D.; Suchard, M.A.; Rambaut, A.; Drummond, A.J. BEAST 2: A Software Platform for Bayesian Evolutionary Analysis. *PLoS Comput. Biol.* **2014**, *10*, e1003537. [CrossRef] [PubMed]
35. Darriba, D.; Taboada, G.L.; Doallo, R.; Posada, D. JModelTest 2: More Models, New Heuristics and Parallel Computing. *Nat. Methods* **2012**, *9*, 772. [CrossRef]
36. Paredes, C.; Huamán, P.; Cardoso, F.; Vivar, R.; Vera, V. Estado Actual Del Conocimiento de Los Moluscos Acuáticos En El Perú. *Rev. Peru. Biol.* **1999**, *6*, 5–47. [CrossRef]
37. Alamo, V.; Valdivieso, V. *Lista Sistemática de Moluscos Marinos Del Perú*, 2nd ed.; Instituto del Mar del Perú: Callao, Peru, 1997.
38. Ramírez, R.; Paredes, C.; Arenas, J. Moluscos Del Perú. *Rev. Biol. Trop.* **2003**, *51*, 225–284.
39. Battaglia, P.; Pedà, C.; Rizzo, C.; Stipa, M.G.; Arcadi, E.; Longo, F.; Ammendolia, G.; Cavallaro, M.; Rao, I.; Villari, A.; et al. How Rare Are Argonautoidea Octopuses in the Mediterranean? New Data from Stranding Events, Stomach Contents and Genetics. *Biology* **2023**, *12*, 420. [CrossRef]
40. Alejo-Plata, M.d.C.; León-Guzmán, S.S.; Díaz-Polo, R.; Torres-Huerta, A.M. Diversity, Abundance and Frequency of Argonauts (Cephalopoda: Argonautidae) in the Diet of Pelagic Fishes of Commercial Value in Oaxaca, Mexico. *Rev. Biol. Mar. Ocean.* **2019**, *54*, 107–117. [CrossRef]
41. Martínez-Soler, E.; Gómez-Gutiérrez, J.; De Silva-Dávila, R.; González-Rodríguez, E.; Aburto-Oropeza, O. Cephalopod Paralarval Species Richness, Abundance and Size Structure during the 2014-2017 Anomalous Warm Period in the Southern Gulf of California. *J. Plankton Res.* **2021**, *43*, 224–243. [CrossRef]
42. Martínez, E. *Variación Temporal de La Estructura de La Comunidad de Paralarvas de Cefalópodos Del Parque Nacional Cabo Pulmo, B.C.S. En Respuesta a La Variabilidad Ambiental (2014–2017)*; La Paz, B.C.S.: La Paz, Mexico, 2019.
43. Nesis, K.N. Cephalopoda. In *South Atlantic Zooplankton*; Boltovskoy, D., Ed.; Backhuys Publishers: Leiden, The Netherlands, 1999.
44. Vecchione, M.; Roper, C.F.E.; Sweeney, M.J.; Lu, C.C. *Distribution, Relative Abundance and Developmental Morphology of Paralarval Cephalopods in the Western North Atlantic Ocean*; US Government Printing Office: Seattle, WA, USA, 2001.
45. Vidal, E.A.; Haimovici, M.; Hackbart, V.C. Distribution of Paralarvae and Small Juvenile Cephalopods in Relation to Primary Production in an Upwelling Area off Southern Brazil. *ICES J. Mar. Sci.* **2010**, *67*, 1346–1352. [CrossRef]
46. Franco-Santos, R.M.; Iglesias, J.; Domingues, P.M.; Vidal, E.A.G. Early Beak Development in *Argonauta nodosa* and *Octopus vulgaris* (Cephalopoda: Incirrata) Paralarvae Suggests Adaptation to Different Feeding Mechanisms. *Hydrobiologia* **2014**, *725*, 69–83. [CrossRef]
47. Cloney, R.A.; Florey, E. Uhrastructure of Cephalopod Chromatophore Organs. *Z. Fiir Zellforsch.* **1968**, *89*, 250–280. [CrossRef]
48. Reed, C.M. The Ultrastructure and Innervation of Muscles Controlling Chromatophore Expansion in the Squid, *Loligo vulgaris*. *Cell Tissue Res.* **1995**, *282*, 503–512. [CrossRef]
49. Messenger, J.B. Cephalopod Chromatophores: Neurobiology and Natural History. *Biol. Rev.* **2001**, *76*, 473–528. [CrossRef]
50. Vecchione, M.; Lipiński, M.R. Descriptions of the Paralarvae of Two Loliginid Squids in Southern African Waters. *S. Afr. J. Mar. Sci.* **1995**, *15*, 1–7. [CrossRef]
51. González, Á.F.; Rocha, F.; Guerra, A.; Bückle, L.; Guerra, A.; Rocha, E.; González, A.E.; Bückle, L.E. Embryonic Stages of the Patagonian Squid Loligo Gahi (Mollusca: Cephalopoda). *The Veliger* **2001**, *44*, 109–115.
52. Barón, P.J. The Paralarvae of Two South American Sympatric Squid: Loligo Gahi and Loligo Sanpaulensis. *J. Plankton Res.* **2003**, *25*, 1347–1358. [CrossRef]
53. Troschel, F.H. Bemerkungen Über Die Cephalopoden von Messina. *Arch. Naturgeschichte* **1857**, *23*, 41–76.